

Tetradehydroadamantane-1,3,5,7-Di- and Tetracations and Their Helium and Hydride Inclusion Complexes: Spherical Aromaticity and Evidence for a Bonding Interaction between Carbon and Helium

Götz Bucher,^{*,†,‡} Felix Köhler,[§] and Rainer Herges[§]

Lehrstuhl für Organische Chemie II, Ruhr-Universität Bochum, Universitätsstrasse 150, 44801 Bochum, Germany, and Institut für Organische Chemie, Christian-Albrechts Universität Kiel, Otto-Hahn-Platz 4, 24098 Kiel, Germany

Received: April 24, 2008; Revised Manuscript Received: July 15, 2008

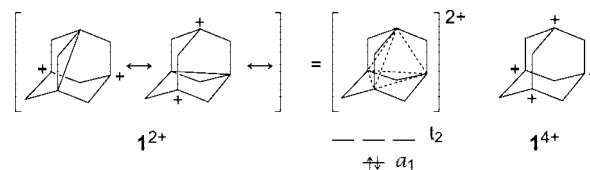
The unusual stability of the experimentally known 1,3-dehydro-5,7-adamantyl dication was previously explained by four-center two-electron aromaticity with three-dimensional (tetrahedral) topology. Magnetic criteria (ACID and ring-current analysis) now demonstrate that there is also a very strong contribution from hyperconjugation with all six methylene bridges. The delocalized system of electrons thus includes all valence electrons, and the structure, therefore, should rather be described as a spherically aromatic 50-electron system. The corresponding T_d -symmetric tetracation with 48 electrons is antiaromatic and not a minimum structure. With a He atom or a hydride ion at the center of the cage, the tetracation is predicted to form a kinetically stable complex. Magnetic criteria demonstrate that the antiaromaticity is greatly reduced, and a bond analysis hints at bonding interactions between He (and H^-) and the carbon atoms of the adamantane cage.

Introduction

According to the Hückel rule, cyclic annulenes show properties characteristic of aromatic compounds if the number of π electrons is given by $z = 4N + 2$. Three-dimensional π systems, however, require $z = 2(N + 1)^2 \pi$ electrons in order to achieve full aromaticity.^{1,2} The electron numbers to fill the spherical cluster shells thus are $z = 2, 8, 18, 32, 50,$ and 72 , which correspond to the magic numbers for the electron configuration in atomic shells. Experimentally determined or calculated ^3He NMR shifts of a helium atom placed in the center of a cage molecule are a measure for its degree of aromaticity.^{3,4} In the case of the He inclusion complex $^3\text{He}@C_{60}$ ($z = 60$), the ^3He NMR shift is $\delta = -6.3$ ppm,³ whereas the decacation $^3\text{He}@C_{60}^{10+}$ ($z = 50$) is predicted to exhibit an extreme ^3He upfield shift of $\delta = -81.4$ ppm, thus indicating a significant increase in aromaticity.¹ A more generally applicable probe for aromaticity that can be conveniently calculated is the nucleus-independent chemical shift (NICS).⁵ Another cage molecule, the 1,3,5,7-didehydroadamantane dication $\mathbf{1}^{2+}$ (Scheme 1), has been predicted to have a nucleus-independent chemical shift (NICS)⁶ at its center of $\delta = -43.0$ ppm, which is indicative of strong aromaticity.⁵

Dication $\mathbf{1}^{2+}$ was prepared and characterized under long-lived stable ion conditions.⁷ Its unusual stability has been attributed to a closed-shell electronic structure with a doubly occupied ($z = 2$) totally symmetric molecular orbital as the HOMO that results from a linear combination of the four p-type atomic orbitals at the bridgehead carbon atoms. Thus, the two electrons form a delocalized system with tetrahedral symmetry that meets the $2(N + 1)^2$ electron count rule of spherical aromaticity. We

SCHEME 1: Structures of $\mathbf{1}^{2+}$ and $\mathbf{1}^{4+}$ and A Simplified MO Scheme of $\mathbf{1}^{2+}$ (including the four p orbitals at the cationic centers)



now use DFT calculations in combination with the anisotropy of induced current density (ACID) method⁸ and current density analyses to shed light on the electronic structure of $\mathbf{1}^{2+}$, the related tetracation $\mathbf{1}^{4+}$, and inclusion complexes derived thereof with He and H^- .

Results and Discussion

In our calculations, dication $\mathbf{1}^{2+}$ was a minimum (in agreement with previous calculations), whereas tetracation $\mathbf{1}^{4+}$ in T_d symmetry turned out to be a triply degenerate third-order saddle point.⁹ The NICS values at the cage centers are $\delta = -46.23$ ppm ($\mathbf{1}^{2+}$) and $\delta = +9.54$ ppm ($\mathbf{1}^{4+}$), indicating that $\mathbf{1}^{2+}$ is aromatic and that the T_d tetracation $\mathbf{1}^{4+}$ might in fact be antiaromatic. This is confirmed by plotting the NICS values in $\mathbf{1}^{2+}$ and $\mathbf{1}^{4+}$ as functions of the distance from the center of the molecule (Figure 1).

In $\mathbf{1}^{2+}$, the NICS value monotonically increases, as would be expected for a spherical aromatic structure. Tetracation $\mathbf{1}^{4+}$, however, exhibits a maximum NICS at a distance of 1.3 \AA from the center. As mentioned above, $\mathbf{1}^{2+}$ previously was described as a two-electron four-center spherically aromatic system. Molecular orbital, ACID, and current density analyses now confirm that, in addition, there is also a strong contribution from hyperconjugation with all six methylene bridges. Each of the three C–C σ bonds and six C–H bonds α and β with respect to each of the cationic centers exhibit the appropriate

* To whom correspondence should be addressed. E-mail: goebu@chem.gla.ac.uk.

[†] Ruhr-Universität Bochum.

[‡] Current address: Department of Chemistry, University of Glasgow, Joseph-Black-Building, University Avenue, Glasgow G12 8QQ, United Kingdom.

[§] Christian-Albrechts Universität Kiel.

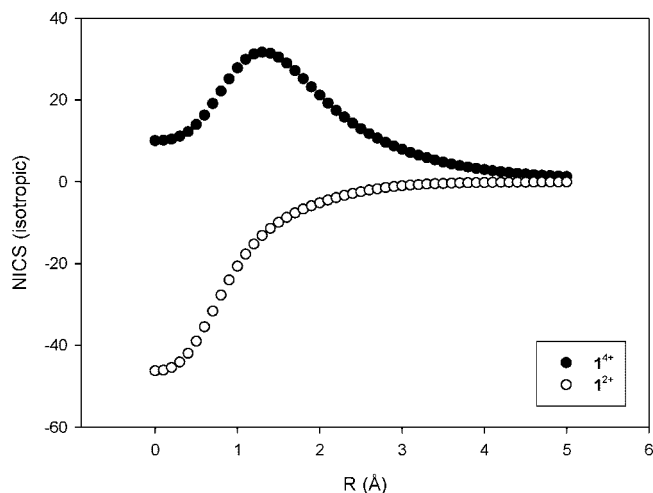
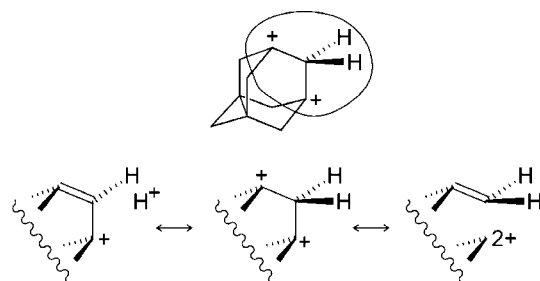


Figure 1. Plot of the NICS values in 1^{2+} and 1^{4+} , calculated at a sequence of points between the center of the tetrahedron ($R = 0$ Å) and a point at $R = 5$ Å along a line connecting the center of the cage with the center of a triangular face (C_3 axis). Open circles, 1^{2+} ; solid circles, 1^{4+} .

symmetry to interact with the empty p orbitals at the sp^2 carbons (Scheme 2).

According to the ACID critical isosurface values (CIVs), the spherical hyperconjugation involving all 50 valence electrons of 1^{2+} far exceeds the two-electron four-center interaction. The CIV values are given in Figure 2, and they quantify the degree of delocalization. With $CIV = 0.025$, the two-electron four-center delocalized system is about one-half as strongly delocalized as the 50-electron system with $CIV = 0.5$. Thus, 1^{2+} is a 50-electron spherical rather than a two-electron four-center aromatic species. Tetracation 1^{4+} likewise should be described as a 48-electron spherical system, which, according to the electron-counting rules $[2(N + 1)^2]$ is not a three-dimensional aromatic system and might, in fact, be three-dimensional antiaromatic.

SCHEME 2: C–H and C–C Hyperconjugation in 1^{2+}



Because the LUMO in 1^{4+} is predicted to be totally symmetric, this species can be expected to be a suitable host for small electron donors with a $1s^2$ configuration such as H^- or He. Both inclusion complexes $He@1^{4+}$ and $H^-@1^{4+}$ are indeed found to be T_d -symmetric minima, which, at least in the case of the He inclusion complex, is surprising in view of the fact that this highly strained species is calculated to be higher in energy by $\Delta H = +147.6$ kcal/mol relative to the separate He atom and 1^{4+} .¹⁰ The barrier for He loss in $He@1^{4+}$ is calculated to be small ($\Delta H^\ddagger = 14.8$ kcal/mol⁹), but it might be large enough for the potential detection of $He@1^{4+}$ in mass spectrometric experiments. The 3He and 1H NMR shifts calculated for the endohedral atoms in the two inclusion complexes are $\delta(^3He) = -23.7$ ppm ($He@1^{4+}$) and $\delta(^1H) = -24.5$ ppm ($H^-@1^{4+}$), which is indicative of some degree of aromaticity.⁶ At the same level of theory, the 3He and 1H NMR shifts are predicted to be $\delta(^3He) = +2.6$ ppm ($He@C_{10}H_{16}$) and $\delta(^1H_{\text{hydride}}) = +14.2$ ppm ($H^-@C_{10}H_{16}$) for the inclusion complexes of He and hydride in neutral adamantane **1**. To elucidate the electronic structures, we applied the ACID method and detailed ring-current analyses to $He@1^{4+}$ and $H^-@1^{4+}$ as well (Figure 3).

$He@1^{4+}$ exhibits a strongly reduced antiaromaticity as compared to that of the empty cage 1^{4+} or even weak aromaticity, which is manifested by a smaller ACID value and a very weak paratropic ring current within the cyclohexane³⁺

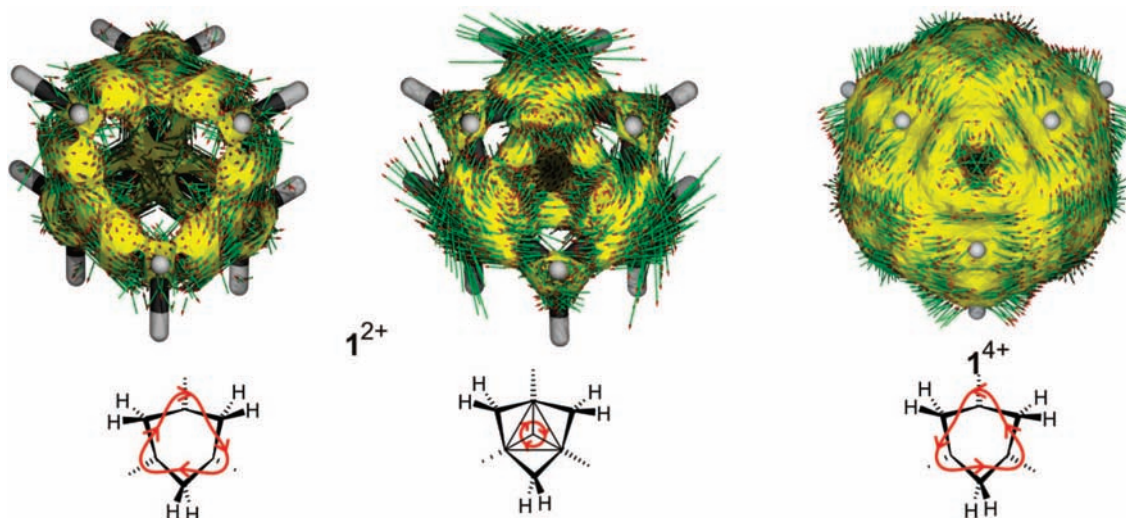


Figure 2. Plots of the anisotropy of induced current density (ACID) for 1^{2+} and 1^{4+} . The magnetic field is parallel to one of the C_3 axes and pointing toward the viewer. The six-ring substructure formed by the three sp^2 carbons and three CH_2 groups is in the front, and one of the cationic centers is at the back. Current density vectors (small green arrows with red arrowheads) are plotted on the ACID surface to visualize the ring currents. The lengths of the arrows are proportional to the current. The ring currents are depicted schematically below each ACID plot. The system of delocalized electrons in 1^{2+} (yellow ACID isosurface, isosurface value 0.05, left plot) includes all C–C and C–H bonds and the current density vectors indicate a diatropic ring current within the six-membered ring substructure. The inner two-electron four-center system of delocalization with a tetrahedral shape is visible only at lower isosurface values (0.025) and only if the ACID calculation is restricted to the HOMO (see ACID plot in the middle). 1^{4+} (plot on the right) exhibits a paratropic ring current (counterclockwise) and therefore is antiaromatic.

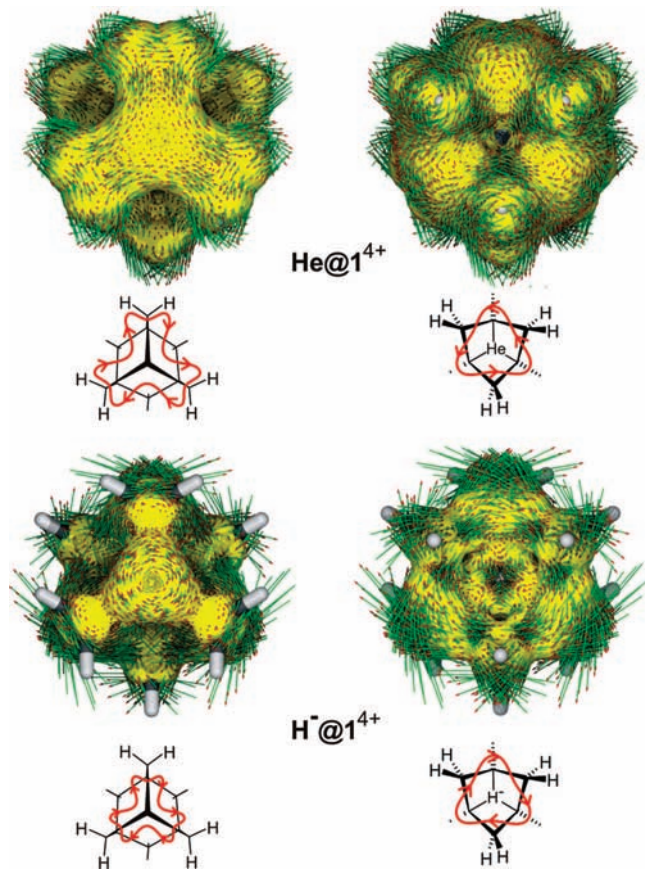


Figure 3. Plots of the anisotropy of induced current density (ACID) and the current density vectors for $\text{He}@1^{4+}$ (top) and $\text{H}^-@1^{4+}$ (bottom). For the relative orientation of the magnetic field and definition of the current density vectors, see Figure 2. The viewing direction is parallel to one of the C_3 axes in two directions: looking onto one of the sp^2 carbons (left) and from the reverse side (perpendicular to one of the six-ring substructures) (right). $\text{He}@1^{4+}$ exhibits a diatropic ring current (clockwise) around the sp^2 carbon and a paratropic ring current within the six-ring subunit (counterclockwise). In $\text{H}^-@1^{4+}$, both ring currents are diatropic.

subunits. Around the sp^2 carbons, a diatropic ring current is observed. The negative ^3He NMR shift (-23.7 ppm) indicates that the diamagnetic contributions more than outbalance the weak paratropic currents. $\text{H}^-@1^{4+}$ exhibits diatropic ring currents in both subunits. This finding is in agreement with the ^1H NMR shift of the central hydrogen atom of $\delta = -24.5$ ppm. $\text{H}^-@1^{4+}$ is thus aromatic. The calculated (B3LYP/6-311++G**//B3LYP/6-31G*) HOMO–LUMO energy gaps in the inclusion complexes are significantly larger than that for empty 1^{4+} , with $\Delta E_{\text{H-L}} = 45.9$ kcal/mol (1^{4+}), 147.9 kcal/mol (1^{2+}), 150.8 kcal/mol ($\text{H}^-@1^{4+}$), and 106.5 kcal/mol ($\text{He}@1^{4+}$).

Interaction of the unoccupied, totally symmetric, linear combination of the four p orbitals at the four sp^2 carbon atoms of 1^{4+} with the $1s^2$ AO of He leads to a C–He bonding MO that is the HOMO – 10 according to a B3LYP/6-311++G**//B3LYP/6-31G* calculated wave function. The antibonding combination forms the LUMO (see Figure 4). The HOMO – 10 has a dominant He $1s^2$ character (small coefficients at the carbon p orbitals) but nevertheless is distinctly distorted toward the four sp^2 C atoms, thus adopting a tetrahedral shape.

As mentioned above, the $\text{He}@1^{4+}$ complex is a minimum on the energy hypersurface, however, it is highly unstable toward dissociation. To estimate the binding forces, we now compare the stability of $\text{He}@1^{4+}$ with that of the neutral $\text{He}@1$ (Table 1).

TABLE 1: Energies^a of 1 , 1^{4+} , $\text{He}@1$, and $\text{He}@1^{4+}$ and of 1 and 1^{4+} Fixed at the Distorted Geometry of the Corresponding He Complexes (1^* and 1^{4+*})^b

$\text{He}@1$	1	He	ΔE_{diss}	
-393.381 286	-390.726 007	-2.907 049	0.251 770	-157.98 kcal/mol
-392.663 584	-390.003 491	-2.900 232	0.240 139	-150.70 kcal/mol
1	1^*		ΔE_{reorg}	
-390.726 007	-390.700 901		0.025 106	15.75kcal/mol
-390.003 491	-389.972 969		0.030 522	19.15kcal/mol
			ΔE_{repuls}	142.23kcal/mol
				131.55kcal/mol
$\text{He}@1^{4+}$	1^{4+}	He	ΔE_{diss}	
-388.463 605	-385.822 314	-2.907 049	0.265 750	-166.76 kcal/mol
-387.745 110	-385.080 066	-2.900 232	0.235 188	-147.6 kcal/mol
1^{4+}	1^{4+*}		ΔE_{reorg}	
-385.822 314	-385.771 590		0.050 724	31.83kcal/mol
-385.080 066	-385.028 614		0.051 452	32.29kcal/mol
			ΔE_{repuls}	134.93kcal/mol
				115.31kcal/mol

^a ΔE_{diss} = dissociation energy, ΔE_{reorg} = strain energy caused by the distortion from the minimum structure of the empty cage to the geometry of the complex. ^b Regular font, B3LYP/6-31G(d); italic font, RCCSD(T)/cc-pVTZ//RCCSD(T)/cc-pVDZ (complexes of 1^{4+}) or RCCSD(T)/cc-pVTZ//B3LYP/6-31G(d) (complexes of 1).

Compared to the neutral complex $\text{He}@1$, the tetracation $\text{He}@1^{4+}$ is less stable toward dissociation but also more strongly distorted with respect to the empty cage. At the CCSD(T) level of theory, the repulsive forces are reduced by 16.2 kcal/mol in $\text{He}@1^{4+}$ as compared to $\text{He}@1$.

The interaction of He with the surrounding cage should also be reflected in the corresponding complex geometries. Whereas the He–CH and He–CH₂ distances in the neutral complex $\text{He}@1$ are 1.627 and 1.848 Å, the corresponding parameters in the tetracationic complex $\text{He}@1^{4+}$ are 1.469 and 1.937 Å. Hence, the He–C distance to the four tertiary carbon atoms decreases by as much as 0.158 Å, and the distance to the methylene bridges increases. This indicates a relative bonding interaction with the cationic centers and stronger repulsion with respect to the methylene bridges. The He–C⁺ interactions obviously are indeed bonding given that the corresponding distance of the center of the cage to the tertiary carbon atoms in the parent adamantane is distinctively larger than the He–C⁺ distance in $\text{He}@1^{4+}$ (Figure 5).

Magnetic criteria indicate a considerable interaction between the central He or H⁻ with the surrounding cage. Now the question arises as to whether this interaction is purely electrostatic or partially covalent in nature. It is little surprising that there is substantial electron transfer between H⁻ and 1^{4+} in the hydride complex. According to atoms in molecules (AIM)¹¹ calculations, the charge at the central hydrogen atom is +0.079 in $\text{H}^-@1^{4+}$. This complex should therefore be more correctly described as $\text{H}^+@1^{3+}$. In the case of the helium complex, the AIM atomic charge at He is +0.052, which indicates only a small degree of charge transfer to the host. The NBO analysis¹² for $\text{He}@1$ predicts very low bond orders for He–CH (0.0483) and He–CH₂ (–0.0209) and a natural charge at He of 0.085, whereas $\text{He}@1^{4+}$ exhibits a distinct bond order for He–C⁺ (0.1527), almost no interaction for He–CH₂ (–0.0080), and a

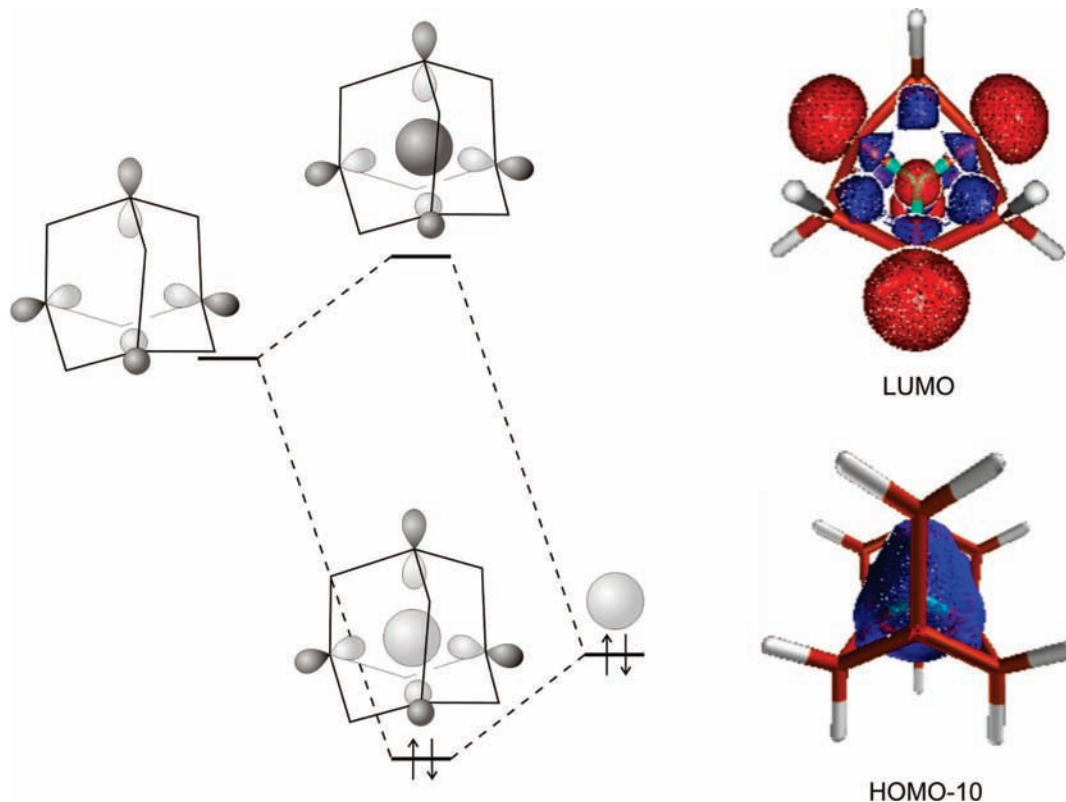


Figure 4. Schematic MO diagram of the interaction of the four p orbitals at the sp^2 carbons with the 1s AO of He (left) and the corresponding MOs plotted from a B3LYP/6-311++G**/B3LYP/6-31G*-calculated wave function (right).

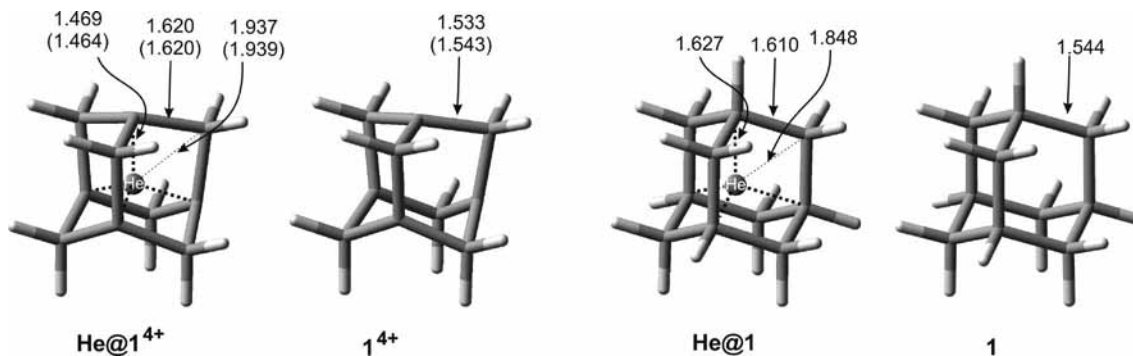


Figure 5. Geometry plots with selected bond lengths (Å) of He@1⁴⁺, 1⁴⁺, He@1, and 1, as calculated at the B3LYP/6-31G(d) level of theory [with RCCSD(T)/cc-pVDZ values in parentheses].

natural charge at He of 0.281. Our calculations thus indicate that bonding between the bridgehead carbon atom and He is significantly more pronounced in He@1⁴⁺ than in He@1. Consistent with this observation, an AIM analysis of the bond path between He and C⁺ in He@1⁴⁺ or H⁻ and C⁺ in H⁻@1⁴⁺ in both cases yields (3, -1) bond critical points (BCPs) between the corresponding pairs of atoms. The electron density (ρ , in au) at this BCP is 0.0906 for He@1⁴⁺ and 0.116 for H⁻@1⁴⁺, which is significantly higher than the corresponding value for the inclusion complexes of He or H⁻ in neutral adamantane, with $\rho = 0.078$ (He)¹³ and 0.0924 (H⁻). The Laplacian [$L = \nabla^2\rho(r_c)$, in au] of the electron density calculated for the C–He (3,-1) BCP in He@1⁴⁺ (H⁻@1⁴⁺) is $L = +0.092$ (+0.018). These values are indicative of a closed-shell interaction.¹¹

How does one account for the aromaticity of 1²⁺ and H⁻@1⁴⁺/He@1⁴⁺ and for the antiaromaticity of *T_d*-1⁴⁺ in terms of electron counting? In view of the strong diatropic or paratropic ring currents involving all C–H and C–C bonds and the strong C–H and C–C delocalization predicted by

the ACID analysis, the complete set of valence electrons has to be included to describe the three-dimensional aromatic properties of these cage molecules (Figure 2). Thus, the total number of delocalized electrons in the dication 1²⁺ is 50, which is a magical number in the $2(N + 1)^2$ rule of three-dimensional aromaticity, and therefore, 1²⁺ is aromatic. The unusual stability of 1²⁺ previously was ascribed to the two-electron four-center aromatic system formed by the four sp^2 carbons.^{2,6,7,14} However, according to our calculations, the aromatic properties of 1²⁺ are dominated by the complete set of all 50 valence electrons. In tetracation 1⁴⁺, the number of delocalized electrons is reduced to 48. Conversely, tetracation 1⁴⁺ would be a 48-electron antiaromatic species. This again is corroborated by its magnetic properties.

In principle, this reasoning could also explain aromaticity of He@1⁴⁺ and H⁻@1⁴⁺, as the sum of valence electrons is also $z = 50$ in both cases. In He@1⁴⁺, the ring current running around the faces of the tetrahedron formed by the four C⁺ atoms is paratropic. This observation indicates that one might have to

treat $\text{He}@1^{4+}$ as a “molecular anion”, with a $z = 2$ aromatic system consisting of a doubly occupied He 1s shell polarized by the extreme electron demand of the surrounding positively charged cage (central five-center two-electron bond) and a $z = 48$ three-dimensional antiaromatic system consisting of the rest of the molecule. In $\text{H}^-@1^{4+}$, both electrons of the hydride are donated to fill the 50-electron three-dimensional aromatic shell of the complex. The trend in aromaticity from 1^{4+} (strongly antiaromatic) through $\text{He}@1^{4+}$ (weakly antiaromatic to weakly aromatic, depending on which criterion of aromaticity is used) to $\text{H}^-@1^{4+}$ (aromatic) goes along with the facility with which He and H^- contribute electrons to the electron demand of the cage.

Computational Methods

All stationary points were fully optimized at the B3LYP/6-31G* level of theory¹⁵ and characterized as minima or transition structures by vibrational analysis. Minima on the tetracation hypersurface were further optimized at the RCCSD(T)/cc-pVDZ level of theory,^{16,17} followed by RCCSD(T)/cc-pVTZ single-point energy calculations based on the RCCSD(T)/cc-pVDZ geometries. In the case of the transition structures and structures derived from neutral adamantane, the RCCSD(T)/cc-pVTZ single-point calculations were based on the B3LYP/6-31G* geometries. Molecular orbitals were obtained by a full population analysis (pop = full) at the B3LYP/6-311++G**//B3LYP/6-31G* level of theory. NMR shifts were calculated at the B3LYP/6-311++G**//B3LYP/6-31G* level of theory employing the gauge-independent atomic orbital (GIAO) method as implemented in Gaussian 03. As reference points, the NMR shifts of a ^3He atom and of tetramethylsilane were calculated at the same level of theory. DFT calculations were performed with the Gaussian 03 suite of programs,¹⁸ whereas Molpro software¹⁹ was used for the RCCSD(T) optimizations and single-point energy calculations. AIM calculations were performed using the AIM2000 program.²⁰ ACID calculations were performed with the ACID program.⁸

Acknowledgment. G.B. thanks H. Bettinger for numerous helpful discussions.

Supporting Information Available: Cartesian coordinates and electronic energies of optimized stationary points. Full citation of ref. This material is available free of charge via the Internet at <http://pubs.acs.org>.

References and Notes

- (1) Hirsch, A.; Chen, Z.; Jiao, H. *Angew. Chem., Int. Ed.* **2000**, *39*, 3915.
- (2) Chen, Z.; Jiao, H.; Hirsch, A.; Thiel, W. *J. Mol. Model.* **2001**, *7*, 161.
- (3) Saunders, M.; Jiménez-Vázquez, H. A.; Cross, R. J.; Mroczkowski, S.; Freedberg, D.; Anet, F. A. L. *Nature* **1994**, *367*, 256.
- (4) Bühl, M.; Thiel, W.; Jiao, H.; Schleyer, P. v. R.; Saunders, M.; Anet, F. A. L. *J. Am. Chem. Soc.* **1994**, *116*, 6005.
- (5) Schleyer, P. v. R.; Maerker, C.; Dransfeld, A.; Jiao, H.; Eikema Hommes, N. J. R. v. *J. Am. Chem. Soc.* **1996**, *118*, 6317.
- (6) Bühl, M.; Kiran, B.; Bremer, M.; Yang, X.; Jiao, H.; Schleyer, P. v. R.; Schreiner, P. R. *Chem. Eur. J.* **2000**, *6*, 1615.
- (7) Bremer, M.; Schleyer, P. v. R.; Schötz, K.; Kausch, M.; Schindler, M. *Angew. Chem., Int. Ed.* **1987**, *26*, 761.
- (8) (a) Herges, R.; Geuenich, D. *J. Phys. Chem. A* **2001**, *105*, 3214. (b) Geuenich, D.; Hess, K.; Koehler, F.; Herges, R. *Chem. Rev.* **2005**, *105*, 3758.
- (9) Relaxation of the geometry without symmetry constraints leads to the tris-2-(propene-3-ylidene)-methyl tetracation in C_3 symmetry (see Supporting Information). At the B3LYP/6-31G* + ZPE level of theory, this species is lower in energy than T_d-1^{4+} by 145.6 kcal/mol.
- (10) Minima: CCSD(T)/cc-pVTZ//CCSD(T)/cc-pVDZ. Transition state: CCSD(T)/cc-pVTZ//B3LYP/6-31G*. Values without ZPE correction.
- (11) Bader, R. F. W. *Atoms in Molecules*; Clarendon Press: Oxford, U.K., 1990.
- (12) Reed, A. E.; Curtiss, L. A.; Weinhold, F. *Chem. Rev.* **1988**, *88*, 899.
- (13) Haaland, A.; Shorokhov, D. J.; Tverdova, N. V. *Chem. Eur. J.* **2004**, *10*, 4416.
- (14) Chan, M. S. W.; Arnold, D. R. *Can. J. Chem.* **1997**, *75*, 192.
- (15) Becke, A. D. *J. Chem. Phys.* **1993**, *98*, 5648.
- (16) Hampel, C.; Peterson, K.; Werner, H.-J. *Chem. Phys. Lett.* **1992**, *190*, 1.
- (17) Kendall, R. A.; Dunning, T. H. *J. Chem. Phys.* **1992**, *96*, 6796.
- (18) Frisch, M. J. et al. *Gaussian 03, revision D.02*, Gaussian, Inc.: Wallingford, CT, 2004.
- (19) *Molpro*, version 2002.6; University of Birmingham: Birmingham, U.K., 1997.
- (20) Biegler-König, F. *AIM 2000*, version 1.0; Bielefeld University of Applied Sciences: Bielefeld, Germany, 1998.

JP803594W